Front. Agr. Sci. Eng. 2025, 12(4): 857–874 https://doi.org/10.15302/J-FASE-2025637

RESEARCH ARTICLE

Enhanced adipogenesis and fatty acid transport in Tibetan pigs compared to Duroc pigs: insights from cellular heterogeneity by scRNA-seq

Jiaping LI*, Sa LI*, Ning LI (✉), Xiaoxiang HU (✉)

State Key Laboratory for Agrobiotechnology, College of Biological Sciences, China Agricultural University, Beijing 100193, China.

*These authors contribute equally to the work

KEYWORDS

Adipocyte development, fat accumulation, fatty acid transport, metabolism capacity, Tibetan pig

HIGHLIGHTS

- scRNA-seq revealed adipocyte heterogeneity and differentiation trajectories.
- Tibetan pigs shown to have higher adipogenic capacity at the mesenchymal stem cell stage.
- Mature adipocytes in Tibetan pigs have enhanced fatty acid transport activity.
- Duroc pigs have stronger oxidative metabolism than Tibetan pigs.

Received January 21, 2025;
Accepted April 24, 2025.

Correspondences: ninglcau@cau.edu.cn, huxx@cau.edu.cn

GRAPHICAL ABSTRACT

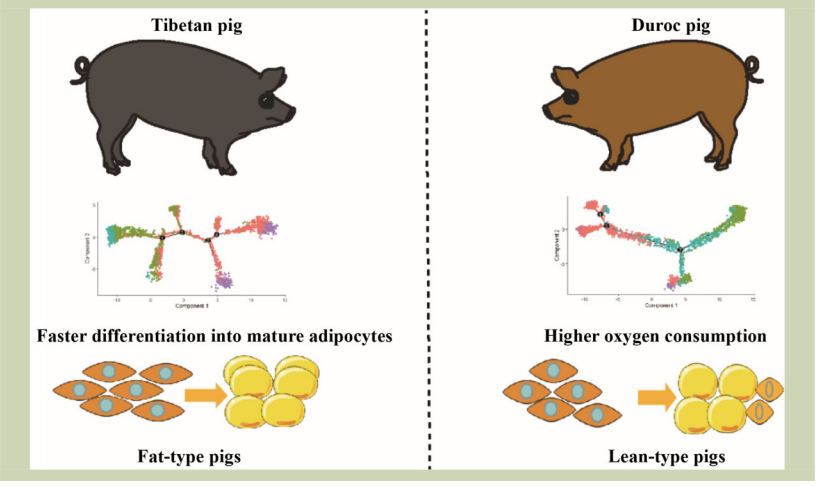

ABSTRACT

Tibetan pigs are known for their excellent fat deposition capacity and greater backfat thickness. In this study, scRNA-seq was performed to reveal the cellular heterogeneity of stromal vascular fraction (SVF) cells within porcine neck adipose tissues. Diverse cell types in neck adipose tissue were identified, including mesenchymal stem cells, preadipocytes, mature adipocytes, macrophages, endothelial cells and vascular smooth muscle cells. Tibetan pigs had a higher proportion of mature adipocytes and a greater tendency for preadipocytes to differentiate into mature adipocytes by pseudo-time analysis. Gene ontology analysis highlighted augment pathways related to fatty acid transport and thermogenesis in Tibetan pigs. *In vitro* experiments further confirmed the superior fat accumulation and fatty acid transport capacities of Tibetan pig SVF cells during adipocyte differentiation, supporting their enhanced fat deposition. Despite their superior adipogenesis, Tibetan pigs had less metabolic activity and oxygen consumption at both the SVF cells and mature adipocyte stages, indicating an adaptation to hypoxic environments at

high elevations. This study provides valuable insights into the mechanisms of fat deposition in pigs and highlights the critical role of Tibetan pig adipose cells in hypoxia adaptation, offering guidance for improving fat content and stress resistance in pig breeding programs.

1 Introduction

Adipose tissue is a critical organ in mammals, with essential functions such as energy storage, cold resistance and regulation of body homeostasis. Adipose tissue development is a dynamic process involving sequential stages of preadipocytes proliferation, differentiation and subsequent adipocyte hypertrophy. In the neonatal period, the preadipocytes undergo committed differentiation into mature adipocytes. The triglycerides accumulation within mature adipocytes leads to lipid droplet enlargement, ultimately results in increased adipose tissue mass and deposition[1]. Adipose tissue can be divided into white adipose tissue (WAT) and brown adipose tissue (BAT). WAT primarily stores excess energy in the form of triglycerides and is distributed across subcutaneous, visceral and epididymal fat depots[2]. In contrast, BAT is mainly found in rodents and infants[3], and is located in regions such as the scapular area, clavicles and axillae[4]. BAT converts chemical energy into heat via non-shivering thermogenesis to resistance cold[5]. There are three types of adipocytes: white, brown and beige adipocytes[6]. White adipocytes contain a unilocular lipid droplet, have few mitochondrial and have low expression of *UCP1*, with their primary function being energy storage[7]. Brown adipocytes have multilocular lipid droplets, are rich in mitochondria, express the classical thermogenic gene *UCP1* at high levels and primarily function to convert chemical energy into heat[8]. Beige adipocytes, distinct cells found within white adipose tissue, share characteristics with brown adipocytes, including multilocular lipid droplets, high mitochondrial content and *UCP1* expression, and are also involved in thermogenesis[9,10].

Both white and beige adipocytes originate from mesenchymal stem cells (MSC), which proliferate and differentiate into preadipocytes. Key adipogenic regulators such as *PPARG* and *CEBPA* drive the differentiation of these preadipocytes into mature white adipocytes, enabling triglyceride storage[4,11]. However, in response to environmental stimuli, such as cold exposure and hormonal signals, MSC differentiate into beige preadipocytes. Under the regulation of the *PRDM16* transcription factor, these preadipocytes differentiate into beige adipocytes, expressing *UCP1* and contribute to thermogenesis[12]. Brown adipocytes and skeletal muscle cells share a common origin from $EN1^{+}/MYF5^{+}$ progenitor cells[12]. *PRDM16* recruits the *CEBPB* transcription factor to promote the differentiation of progenitor cells into brown adipocytes[4]. The SVF cells derived from adipose tissue comprises a variety of cell types and have significant cellular heterogeneity, including MSC, preadipocytes, vascular endothelial cells (VEC), fibroblasts and immune cells. Of these, MSC and preadipocytes are crucial for promoting adipocyte proliferation and regulating angiogenesis, thereby contributing to adipose tissue expansion and fat deposition[13]. Recent studies have demonstrated that SVF cells isolated from neonatal mice can form adipose spheroids and secrete *LEPTIN in vitro*, it can also respond to adrenergic lipolytic stimulation, further supporting their essential role in adipogenesis[14]. In human adipose tissue, three distinct progenitor cell types within the SVF cells have been identified, which can differentiate into preadipocytes and subsequently mature adipocytes, thus promoting lipid accumulation[15]. Also, scRNA-seq of adipose-derived stem cells (ADSC) from women with pear-shaped and apple-shaped obesity revealed depot-specific adipogenic potential; abdominal ADSC preferentially differentiate into adipocytes promoting fat accumulation whereas gluteal ADSC are more associated with lipid and cholesterol metabolism[16]. Collectively, SVF cells includes multiple cell types and early lineage markers involved in adipocyte differentiation and adipose tissue expansion, supporting its critical role in regulating fat deposition.

Due to the absence of brown adipose tissue and a functional *UCP1* gene in pigs, white adipose tissue becomes the primary fat organ, having a key role in regulating metabolic processes[17]. Based on body fat percentage and lean meat content, pigs are generally classified as either fatty or lean types. Tibetan pigs, a typical fatty breed, inhabit high-elevation regions at about 2800 and 4000 m above sea level. To adapt to the harsh conditions of cold and hypoxia at these elevations, adult Tibetan pigs have significantly higher fat content and backfat thickness compared to Duroc pigs, with an average fat percentage of 41% and backfat thickness of 2.59 cm[18]. In our study, we focused on the Diqing Tibetan pig, a high-elevation breed in China known for its exceptional fat deposition, thick backfat, and superior meat quality traits[19]. In contrast, Duroc

pigs, a globally recognized lean-type breed, are extensively used as sires in crossbreeding programs to improve the production performance of other pig breeds[20]. Adult Duroc boars have a lean meat percentage of 65% and a backfat thickness of around 1.5 cm[21]. As a representative Chinese indigenous pig breed, Tibetan pigs have significantly higher intramuscular fat content compared to the commercial Duroc pigs[22]. Studies on porcine adipose tissue have demonstrated that adipose tissue growth predominantly relies on adipocyte hyperplasia during early developmental stages, characterized by the proliferation and differentiation of MSC into mature adipocytes. Meishan pigs, a representative fatty breed, have significantly larger adipocytes and thicker backfat than lean-type breeds such as Landrace. Notably, differences in backfat thickness between Meishan and Landrace pigs are evident as early as 1 week of age, with Meishan pigs having both a greater number and larger size of adipocytes[23]. Meishan pigs consistently have thicker backfat and more advanced adipose development than Landrace pigs with same bodyweight[24], it is suggested that early adipocyte morphology is closely associated with subsequent fat deposition. Similarly, in intramuscular adipose tissue, Wujin pig is a fat-type breed and it has larger intramuscular adipocytes than Landrace pigs. Local pig breeds generally have larger adipocytes and earlier adipogenic maturation than commercial breeds[25], indicating that the degree of early adipocyte development could a crucial determinant for the extent of fat accumulation during later stages of growth. To explore the differences in adipocyte development between Tibetan and Duroc pigs, we conducted investigated the heterogeneity of their adipose tissues.

scRNA-seq technology is widely used to reveal cellular heterogeneity within tissues. Unlike flow cytometry, which is limited by the availability of antibodies and its sorting capacity, scRNA-seq allows for the detection of all cell types within a tissue sample. For example, scRNA-seq has been applied to mouse adipose tissue, where it identified a novel population of *DPP4*$^+$ MSC capable of differentiating into preadipocytes[26]. Additionally, *CD81*$^+$ preadipocytes were observed to differentiate into thermogenic beige adipocytes under cold stimulation in mouse inguinal white adipose tissue, as revealed by scRNA-seq analysis[27]. In human adipose tissue, scRNA-seq identified cellular heterogeneity and had an increase in immune cell populations with enhanced metabolic activity in obese individuals[28]. As scRNA-seq technology continues to evolve, it has provided deeper insights into cellular heterogeneity in various tissues, including mouse brain neural cells, cardiac tissue and human spermatogenesis[29–31].

However, the cellular heterogeneity of adipose tissue in pigs, a significant agricultural animal, remains poorly understood. In this study, we investigated the cellular heterogeneity in the neck white adipose tissue of pigs and explored the differences in adipogenesis between Tibetan and Duroc pigs. Given the significant disparity in fat content between Tibetan and Duroc pigs[18,21], we hypothesized that there may be differences in the proportion of adipocytes within their adipose tissues, as well as in the proliferation and differentiation capacities of SVF cells. These differences could potentially contribute to the increased fat deposition observed in Tibetan pigs.

2 Materials and methods

2.1 Animal sources and adipose tissue collection

Three 4-day-old male Diqing Tibetan pigs were purchased from Yunnan Agricultural University in China and three 4-day-old male Duroc pigs were obtained from the Pig Breeding Farm (Beijing Zhongyu, China). After 12 h of fasting with free access to water, anesthesia was administered via ketamine injection, followed by exsanguination through the anterior vena cava. The carcasses were then cleaned with water and 75% ethanol. Subcutaneous white adipose tissue from the neck and inguinal regions was immediately collected and placed in 1.5 mL centrifuge tubes, flash-frozen in liquid nitrogen, and stored at −80 °C. Some adipose tissue samples were preserved in 4% paraformaldehyde solution and stored at 4 °C. The remaining subcutaneous white adipose tissue from the neck and inguinal regions was placed in high-glucose DMEM for SVF cell isolation.

2.2 Cell isolation and culturing

The adipose tissue from each pig was removed from the DMEM solution, briefly rinsed in 75% ethanol for 2 s, and then placed in phosphate buffered saline (PBS) within a sterile laminar flow hood. The tissue was minced into a homogenous, meat-like consistency. All minced tissues were added to HEPES buffer (Gibco, Thermo Fisher Scientific, Waltham, MA, USA) containing collagenase II (Gibco) at a final concentration of 0.2% (w/v) and incubated at 37 °C with shaking for 45 min. After digestion, an equal volume of cell culture medium consisting of high-glucose DMEM (Gibco), 200 U·mL^{-1} penicillin/streptomycin (Gibco), and 10% FBS (Gibco), then it was added to terminate collagenase activity. The mixture was then sequentially filtered and the collected solution was centrifuged. The resulting pellet contained SVF cells. Red blood cells were removed by adding red blood cell lysis buffer (Beyotime, Beyotime Biotech Inc, Haimen, Jiansu, China),

followed by centrifugation. The isolated cells from each pig were resuspended in cell culture medium in 6-well plates. After incubating for 2 h at 37 °C to allow for cell adhesion, the medium was replaced and the cells further cultured for 3 days. Subsequently, a portion of the cells was maintained in culture for further experiments, while the remaining cells were cryopreserved in liquid nitrogen for future use.

2.3 Preparation of single-cell suspensions and cDNA library construction

After culturing the SVF cells for 1 day, a portion of the cells was collected using 0.25% trypsin digestion (Gibco). The SVF cells from three Tibetan pigs and three Duroc pigs were then separately mixed. After centrifugation at 1000 r·min^{-1}, the pellet was resuspended in 0.04% bovine serum albumin and filtered through a 40 μm cell strainer to remove large cell fragments and debris. A 10 μL sample of the cell suspension was mixed with 10 μL of Trypan blue (Invitrogen, Thermo Fisher Scientific) and counted using the Countness II Automated Cell Counter. The cell concentration was adjusted to 700–1200 cells μL^{-1}, ensuring a viability of over 80%. Single-cell gel beads in emulsion (GEMs) were prepared using the 10x Genomics Chromium Controller Instrument (Genomics Ltd., Oxford, UK), following the 10x Genomics protocol.

To obtain 10,000 cells for library construction, 10.2 μL of single-cell suspension from Tibetan pigs and 21.8 μL from Duroc pigs were combined and diluted with nuclease-free water to a final volume of 33.9 μL, following the 10x Genomics protocol (Genomics). The resulting single-cell suspension was then mixed with a master mix and loaded into the 10x Genomics Chromium Controller Instrument to produce GEMs. Subsequently, the GEM-RT program and cDNA amplification were performed to construct the cDNA library. The cDNA library was purified and size-selected according to the manufacturer's protocol (Genomics), and quality was assessed using the Agilent 2100 Bioanalyzer System (Agilent, Santa Clara, CA, USA). The qualified library was then sequenced by BGI Genomics.

2.4 Detection of cell proliferation

According to the protocol of a BeyoClick EdU Cell Proliferation Kit with Alexa Fluor 488 (Beyotime), SVF cells from Tibetan and Duroc pigs, with equal volumes of cell suspension, were seeded separately into three replicate wells each of a 12-well plate and a 6-well plate, and cultured for 24, 48 and 72 h. After each time point (24, 48 and 72 h), cells in the 6-well plate were used for Hoechst nuclear labeling, while those in the 12-well plate were used for cell proliferation detection.

To perform nuclear labeling, prewarmed EdU working solution was added to the cells in three replicate wells of the 6-well plate at a final concentration of 1×. The cells were incubated at 37 °C for 2 h. After incubation, the cell culture medium was removed and 1 mL of 4% paraformaldehyde added to fix the cells. Following fixation, the cells were washed with buffer and permeabilized with Triton X-100 for 15 min. The Click Additive Solution, prepared using the reagents provided in the kit, was then added to cover the cells. After incubating in the dark for 30 min, Hoechst 33342 (provided in the kit) was used for nuclear staining, and the cells were imaged under a microscope.

For the CCK-8 assay, the CCK-8 solution from a Cell Counting Kit-8 (Beyotime,) was added to the cells in three replicate wells of the 12-well plate, containing cells from both Tibetan and Duroc pigs, at 24, 48, and 72 h. After incubating at 37 °C for 4 h, the absorbance values were measured at 450 nm using the Tecan Infinite F50 machine (Tecan, Männedorf, Switzerland).

2.5 Adipogenesis of SVF cells

Adipose SVF cells from Tibetan and Duroc pigs were cultured in adipogenesis medium in a 12-well plate, with three replicate wells for each group. The adipogenesis medium consisted of 4 nmol·L^{-1} insulin, 10 mmol·L^{-1} HEPES and 4 mmol·L^{-1} glutamine[32]. The medium was refreshed every other day. On day 8, cells were collected using TRIzol for RNA extraction.

2.6 Oil red O staining and lipid content measurement

The cells from Tibetan and Duroc pigs with three replicate wells were differentiated on day 8, the cells were washed for three times with PBS and subsequently fixed with 4% paraformaldehyde at room temperature for 15 min. Concurrently, an Oil Red O working solution was prepared by dissolving oil red O powder (Sigma, Washington, DC, UAS) in isopropanol, followed by mixing with deionized water in a 3:2 ratio and double filtration before use. After removal of paraformaldehyde, the cells were incubated with the Oil Red O working solution at room temperature for 20 min, followed by PBS washing until the red color disappeared. Images were captured under a microscope.

For lipid content quantification, PBS was removed, and 100%

isopropanol was added to both the samples and blanks, followed by incubation at room temperature for 15 min. Subsequently, absorbance values were measured at 510 nm[33].

2.7 RT-qPCR

A 500-ng sample of total RNA was reverse-transcribed into cDNA using a PrimeScript RT reagent kit with gDNA Eraser (Takara, Kyoto, Japan). The cDNA was diluted with water and used for qPCR analysis. The RT-qPCR reaction mixture was prepared using TB Green Premix Ex Taq (Takara). Briefly, 0.4 μL of primers as shown in Table S1 were dissolved in the reagent of TB Green Premix Ex Taq to achieve a final concentration of 0.2 μmol·L^{-1}. Subsequently, 2 μL of cDNA was added to a total reaction volume of 20 μL.

The mixture was loaded into a 96-well plate and subjected to qPCR using the 7300 Fast Real-Time PCR System (Applied Biosystems, Foster City, CA, UAS). The thermal cycling program included an initial denaturation step at 95 °C for 30 s, followed by 40 cycles of denaturation at 95 °C for 5 s and annealing/extension at 60 °C for 30 s. Expression values were normalized to 18S mRNA levels. Relative mRNA expression was determined using the $^{\Delta\Delta}$Ct method.

2.8 Cell oxygen consumption detection

On day 3, cells were transferred to Agilent Seahorse XF24 Cell Culture Microplates (Agilent) at a density of 10,000 cells per well and continued to differentiate in adipogenesis medium for 4 days. On day 7, XFe24 FluxPak plates (Agilent) were pre-incubated in a non-CO_2 incubator for calibration, preparing them for the experiment.

On day 8, oligomycin, FCCP (carbonyl cyanide-p-trifluoromethoxyphenylhydrazone) and a mixture of antimycin A and rotenone were added to the XFe24 FluxPak plates (Agilent) at final concentrations of 1, 2 and 2 μmol·L^{-1}, respectively. The cell medium was then replaced with Seahorse XF Assay medium (Agilent) including 4.5 mg·mL^{-1} glucose (Gibco), 1mM Sodium pyruvate (Gibco) and 1x GlutaMax (Gibco). The plates were then placed in a non-CO_2 incubator. After calibration and equilibration of the XFe24 FluxPak plates in the Seahorse XFe24 Analyzer, the Agilent Seahorse XF24 Cell Culture Microplates were used to measure oxygen consumption capacity. At the end of the experiment, oxygen consumption data from each group (with five replications) were statistically analyzed and graphed.

2.9 Histological analysis

Adipose tissue was embedded in paraffin and sectioned into 5 μm slices. The slices were then placed in a heater at 68 °C for 1 h to melt the paraffin. Following this, xylene and ethanol with different concentrations were used to remove the paraffin. For staining, the slices were sequentially stained with hematoxylin and eosin to visualize nuclear and cytoplasmic features. The slices were processed by gradient dehydration with increasing concentrations of ethanol. Finally, xylene and neutral resin were used to mount coverslips on the slices. Three replicate slices from each pig were examined and images were taken at least three times per slice using a microscope.

2.10 Analysis of scRNA-seq data

Single-cell RNA sequencing data were processed using the Cell Ranger Single Cell Software Suite (v3.0.2; Genomics) and Seurat v3.1.2[26]. This pipeline included sample demultiplexing, read alignment, filtering, unique molecular identifier (UMI) counting, inter-sample normalization and unsupervised clustering. Cell cluster visualization was performed using Loupe Cell Browser (v3.0; Genomics). Dimensionality reduction and clustering were based on principal component analysis (PCA) with the top 20 variable genes, followed by visualization using t-distributed stochastic neighbor embedding (t-SNE) with resolution of 0.5 for clustering.

Pseudo-time trajectory analysis was conducted with Monocle 3 using default parameters. Clusters associated with adipocyte development were identified based on the t-SNE plot and corresponding barcodes were extracted. Dimensionality reduction was performed using the DDRTree method via the *reduceDimension* function with max_components set to 2, and cell ordering was achieved accordingly. Significant genes driving cell ordering were identified using the *differentialGeneTest* function, and cells were subsequently arranged along the inferred developmental trajectory.

Differentially expressed genes (DEGs) were identified using a threshold of $P \leqslant 0.05$ and fold change > 2. Cell types were annotated based on known marker genes and DEGs. Functional enrichment of DEGs was conducted using the Metascape platform (metascape.org) for gene ontology (GO) analysis.

To assess differences in cell-type composition between Tibetan and Duroc pigs, the total number of cells from each pig breed was compared. The proportional change in each cell cluster was calculated by subtracting the number of cells in a given

cluster from Duroc pigs from that of Tibetan pigs, followed by normalization to the total cell number in Duroc pigs to obtain the relative change in cell-type proportion.

3 Results

3.1 Tibetan pigs had greater adipogenic capacities in white adipose tissue than Duroc pigs

To elucidate the biological characteristics of WAT in Tibetan and Duroc pigs, subcutaneous WAT was collected from the necks of 4-day-old Tibetan and Duroc pigs and performed histological analysis using hematoxylin and eosin staining. We observed that both Tibetan and Duroc adipocytes contained unilocular large lipid droplets in WAT, with some multilocular lipid droplet cells present among the white adipocytes Fig. 1(a).

We analyzed genes involved in adipogenesis and found that the expression of the early adipogenic regulator genes *CEBPA* and *CEBPB* was significantly higher in Tibetan pigs than in Duroc pigs Fig. 1(b). Additionally, *Leptin* expression was significantly

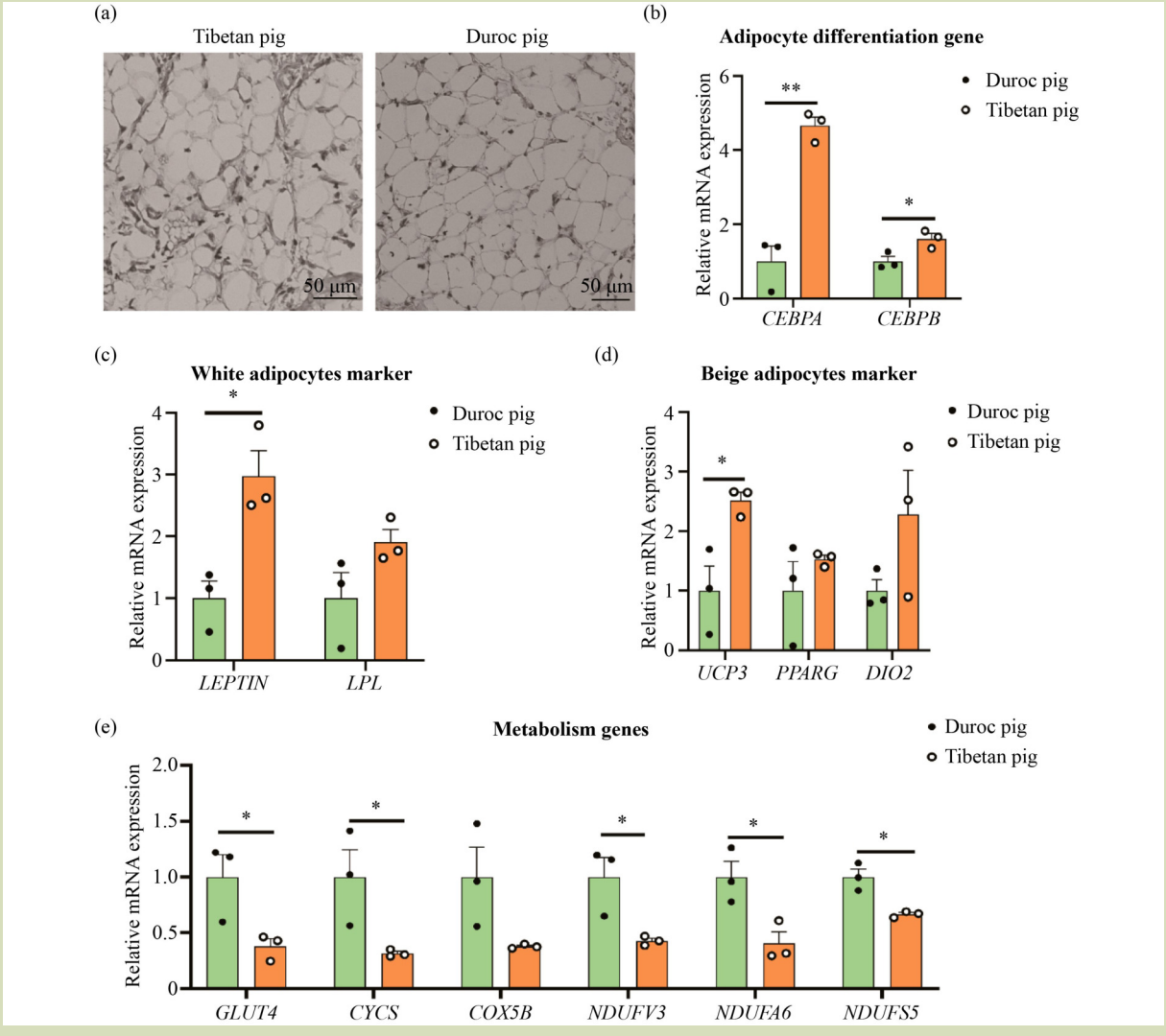

Fig. 1 Adipocyte morphology and gene expression in neck WAT from Tibetan and Duroc pigs. (a) Hematoxylin and eosin staining of neck WAT in 4-day Tibetan and Duroc pigs (scale bar 50 μm). (b) Detection of adipogenesis genes expression in neck WAT from Tibetan and Duroc pigs. (c) Detection of white adipocytes marker expression in neck WAT from Tibetan and Duroc pigs. (d) Detection of beige adipocytes marker expression in neck WAT from Tibetan and Duroc pigs. (e) Detection of metabolism genes expression in neck WAT from Tibetan and Duroc pigs. For qPCR detection, each group included three biological replicates from Tibetan and Duroc pigs (n = 3). Statistical significance was calculated on these mean values by t-test, * $P < 0.05$. ** $P < 0.01$.

elevated in Tibetan pigs Fig. 1(c). *PPARG* contributes to thermogenesis and the induction of browning of WAT[34]. We also assessed the expression of beige adipocyte marker genes, including *PPARG*, *DIO2* and *UCP3*, and found that *UCP3* expression was higher in Tibetan pigs than in Duroc pigs Fig. 1(d). However, glucose transporter and mitochondrial gene expressions were significantly higher in Duroc pigs than in Tibetan pigs Fig. 1(e).

These findings indicate that Tibetan pigs had significantly higher adipogenic capacity but lower metabolic activity than Duroc pigs.

3.2 Single-cell sequencing revealed the SVF cells heterogeneity in subcutaneous adipose tissue from Tibetan and Duroc pigs

To understand adipocyte development in Tibetan and Duroc pigs, we performed scRNA-seq to uncover the SVF cells heterogeneity in subcutaneous WAT. SVF cells were isolated from neck WAT and cultured in a 6-well plate for 1 day. The cell viability of Tibetan pig was 95% and of Duroc pig was 86% as shown in Table S2. Subsequently, single-cell transcriptome library construction was performed, followed by sequencing. DNA libraries were evaluated and optimal fragment sizes ranging from 350 to 1200 bp were selected for sequencing (Fig. S1(a)).

Sequencing yielded around 480 million reads for both Tibetan and Duroc pigs. Tibetan pig generated 9874 cells with a mean of 50,018 reads per cell, a median of 3236 genes per cell, a median of 17,179 UMI counts per cell and a total of 16,352 detected genes as shown in Table S2. Duroc pig obtained 9051 cells with a mean of 53,335 reads per cell, a median of 3504 genes per cell, a median of 19,532 UMI counts per cell and a total of 16,090 detected genes as shown in Table S2. Subsequently, cell clustering was performed after removing low-quality cells based on criteria including a mitochondrial proportion exceeding 25%, nFeature-RNA less than 200 and greater than 4500, Fig. S1(b,c).

We identified 12 clusters in Tibetan pigs and 11 clusters in Duroc pigs through t-SNE clustering Fig. 2(a,c) and named them based on different expressed genes and marker genes as shown in Table S3 and Table S4.

We defined clusters expressing *CD34* in Tibetan and Duroc pigs as mesenchymal stem cells (MSC), Fig. 2(b,d). Previous studies have found the expression of *CD34* in progenitor cells isolated from porcine subcutaneous adipose tissue[35]. *CD34* has also been used as a marker for MSC in human adipose tissue[36]. We identified the cluster with high *CD44* expression as adipose stem cells (ASC), Fig. 2(b,d) because *CD44* is commonly used as a marker gene to identify and isolate mouse ASC[37,38]. Here, we name clusters expressing *CD44* and *CD142* as preadipocytes Fig. 2(b,d). *Cd142* is a newly discovered marker gene for preadipocytes, used in single-cell sequencing of mice to identify preadipocytes[26]. In human adipose tissue, $CD26^{+}$ adipocyte stem cells express *CD142*[39]. In addition, we also identified clusters specifically expressing *ADIPOQ* as mature adipocytes and clusters with specific proliferation marker gene *MKI67* as proliferating cells, Fig. 2(b,d)).

For clusters in Tibetan and Duroc pigs without differentially expressed genes, we could not define cell types and thus named them as unknown clusters. In Tibetan pigs, we extracted upregulated genes from the unknown cluster and performed GO analysis to understand their functions. We found that the regulation of protein catabolic processes, organelle biogenesis and maintenance and organelle assembly pathways were upregulated, Fig. S2(a). Similarly, for the unknown cluster in Duroc pigs, we performed GO analysis on upregulated genes and found that pathways related to the negative regulation of cell proliferation, extracellular matrix organization, and inflammatory response were enhanced, Fig. S2(b).

3.3 Mature adipocytes numbers were greater in Tibetan than in Duroc pigs

We compared the SVF cell heterogeneity between Tibetan and Duroc pigs and observed distinct differences. In Tibetan pigs, we identified separate clusters for proliferation and MSC, proliferation, VEC, myoblasts. In contrast, Duroc pigs had a single cluster combining myoblasts and VEC, while MSC formed a distinct cluster. Notably, Tibetan pigs lacked the MAC cluster, Fig. 3(a).

Tibetan pigs had an increased proportion of mature adipocytes, oxidative metabolism cells, proliferation and preadipocytes, endothelial cells clusters. Conversely, the proportion of proliferation and ASC, preadipocytes, VSMC and MSC clusters decreased in Tibetan pigs more than in Duroc pigs, Fig. 3(a,b).

To study the adipocyte development in Tibetan and Duroc pigs, we extracted cell population by marker genes at different stages of adipose development. *CD34*, *CD44*, *CD142* and *ADIPOQ* were used to identify MSC, ASC, preadipocytes, mature adipocytes, respectively. Therefore, we found that $ADIPOQ^{+}$ cells numbers were greater whereas the $CD34^{+}$ cells,

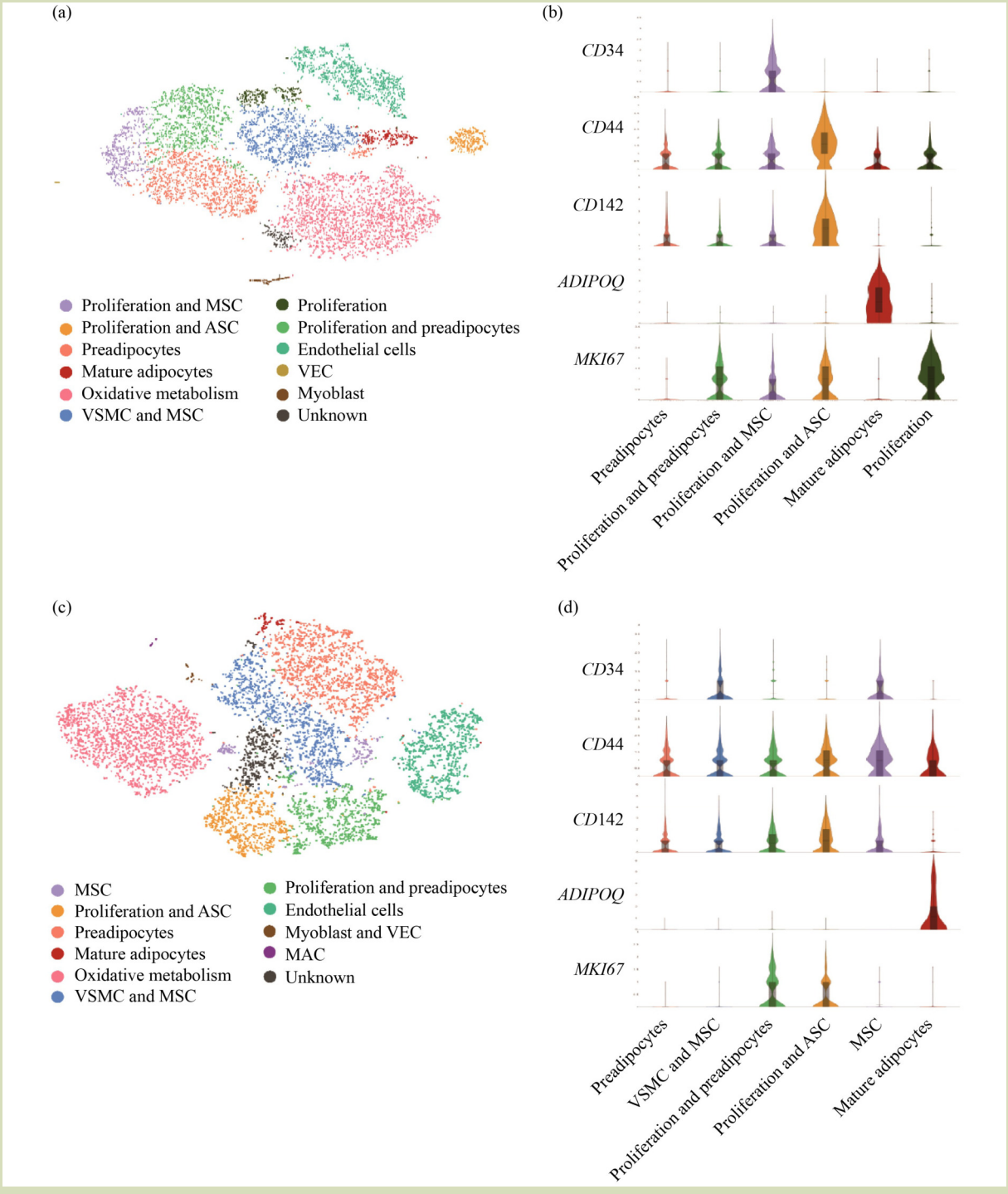

Fig. 2 Identification of cell types in SVF cells of neck WAT by scRNA-seq analysis. (a) t-SNE clustering revealed 12 clusters based on differently expressed genes expression from 9874 SVF cells in Tibetan pigs. (b) Violin plot of adipogenesis and proliferation genes in preadipocytes, proliferation and preadipocytes, proliferation and MSC, proliferation and ASC, mature adipocytes and proliferation clusters from Tibetan pig. (c) t-SNE clustering revealed 11 clusters based on differently expressed genes expression from 9051 SVF cells in Duroc pigs. (d) Violin plot of adipogenesis and proliferation genes in preadipocytes, VSMC and MSC, proliferation and preadipocytes, proliferation and ASC, MSC, mature adipocytes from Duroc pig. ASC, adipose stem cells; MAC, macrophages; MSC, mesenchymal stem cells; VEC, vascular endothelial cells; and VSMC, vascular smooth muscle cells.

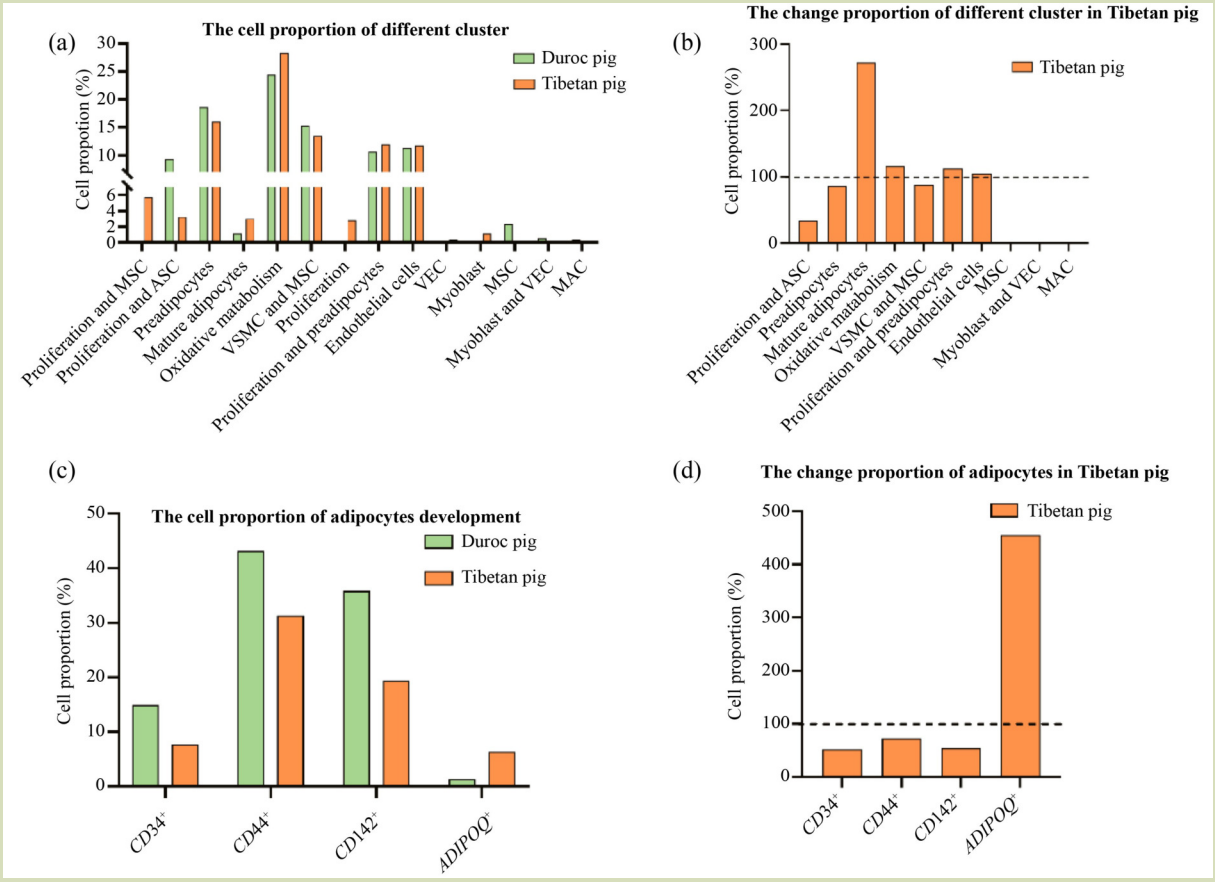

Fig. 3 Cell proportion counted of different clusters from Tibetan and Duroc pigs. (a) Cell proportion of all clusters in SVF cells from Tibetan and Duroc pigs. (b) Changed cell proportion of different clusters in SVF cells from Tibetan compared to Duroc pigs. (c) Cell proportion of clusters related to adipocyte development in SVF cells from Tibetan and Duroc pigs. (d) Changed cell proportion of clusters related to adipocyte development in SVF cells from Tibetan compared to Duroc pigs.

CD44$^+$ cells and *CD142*$^+$ cells were fewer in Tibetan pigs than in Duroc pigs, Fig. 3(c,d).

3.4 A greater proportion of stem cells differentiated into mature adipocytes in Tibetan than in Duroc pigs

To investigate the adipocyte differentiation process in Tibetan and Duroc pigs, we conducted a pseudo-time analysis Fig. 4(a,b). In Tibetan pigs, the proliferation and ASC cluster served as the starting point for adipose differentiation. This cluster bifurcated into two branches, reaching Branch Point 1, where cells went into proliferation cells and preadipocytes. Subsequently, at Branch Point 3, some cells continued to remain in the proliferation and preadipocytes states, while others progressed through Branch Points 2 and 4 to go to mature adipocytes. Additionally, some cells persisted in the preadipocytes state Fig. 4(a).

In Duroc pigs, the proliferation and ASC cluster also as the starting point for adipose differentiation, differentiated into three directions at Branch Point 2. Some cells went to proliferation and preadipocytes, while others become preadipocytes, with a minority eventually differentiated into mature adipocytes. In addition, some cells went into preadipocytes at Branch Point 3, and some cells maintained at ASC state Fig. 4(b).

3.5 Fatty acid transporters and thermogenesis pathways were upregulated during adipocyte differentiation in Tibetan pigs

In addition, we selected upregulated genes in Tibetan and Duroc pigs from all clusters by aggregated scRNA-seq analysis (Fig. S3) and performed GO analysis, Fig. 4(c,d)). In Tibetan pigs, compared to Duroc pigs, pathways related to actin cytoskeleton organization, VEGFA-VEGFR2 signaling, fatty

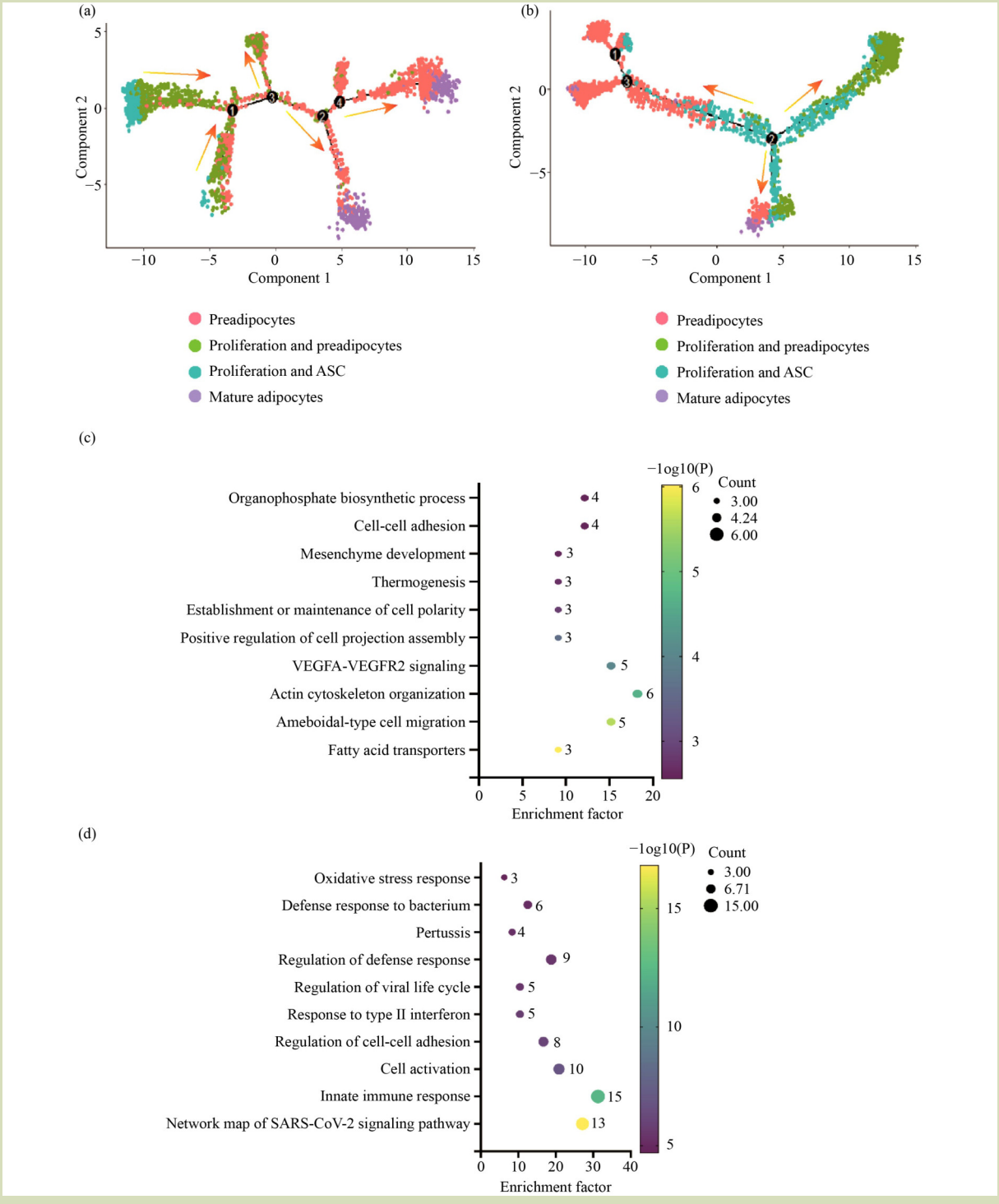

Fig. 4 Pseudo-time analysis of clusters and GO analysis of upregulated genes in Tibetan and Duroc pigs. (a) Pseudo-time analysis of clusters during adipocyte development in Tibetan pigs. Red arrows indicate the differentiation direction of cells. The differentiation state altered through Branch Points 1, 2, 3 and 4. (b) Pseudo-time analysis of clusters during adipocyte development in Duroc pigs. Red arrows indicate the differentiation direction of cells. The differentiation state altered through Branch Points 1, 2 and 3. (c) Upregulated pathway in Tibetan pigs by GO analysis from upregulated genes in all clusters compared to Duroc pigs. (d) Upregulated pathway in Duroc pigs by GO analysis from upregulated genes in all clusters compared to Tibetan pigs.

acid transporters and thermogenesis were upregulated, Fig. 4(c). In Duroc pigs, compared to Tibetan pigs, pathways related to the innate immune response, cell activation and regulation of defense response were upregulated, Fig. 4(d).

Subsequently, we used *CD34*, *CD44*, *CD142* and *ADIPOQ* to indicate different stages of adipogenic differentiation to study the process of fat deposition in Tibetan pigs. We selected *CD34*$^+$ cells from the integrated data and considered them as representing the MSC state. We extracted the upregulated genes in Tibetan pigs for comparison with Duroc pigs and conducted GO analysis. In Tibetan pigs, we found upregulated pathways, including the negative regulation of growth, fatty acid transporters and thermogenesis, Fig. 5(a).

Next, we selected *CD44*$^+$ cells to represent the state of ASC. We extracted the upregulated genes in Tibetan pigs for comparison with Duroc pigs and performed GO analysis. In Tibetan pigs, we observed upregulated pathways including fatty acid transporters, regulation of actin filament-based processes, thermogenesis and negative regulation of cell population proliferation, Fig. 5(b). We extracted the upregulated genes in Tibetan pigs from *CD142*$^+$ cells as the state of preadipocytes and performed GO analysis. Compared to Duroc pigs, we observed that pathways related to fat development, such as fatty acid transporters, thermogenesis and positive regulation of lipid localization, were upregulated in Tibetan pigs, Fig. 5(c).

Finally, we selected upregulated genes in Tibetan pigs from *ADIPOQ*$^+$ cells as the state of mature adipocytes and performed GO analysis. In Tibetan pigs, compared to Duroc pigs, we observed enhanced pathways including fatty acid transport, regulation of plasma membrane-bound cell projection organization and VEGFA-VEGFR2 signaling, Fig. 5(d).

These findings indicate that the adipose SVF cells of Tibetan pigs possessed greater adipogenic potential and had enhanced thermogenic capacity compared to those of Duroc pigs.

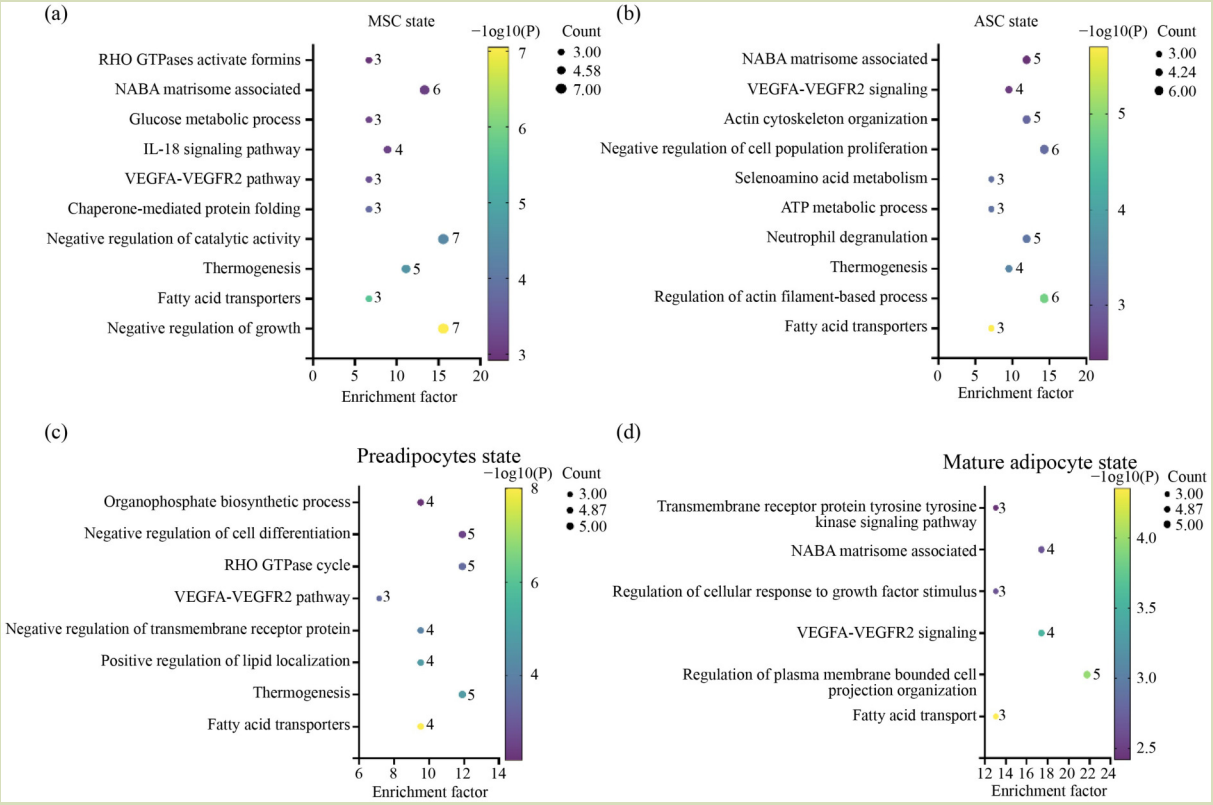

Fig. 5 GO analysis of upregulated genes in Tibetan pigs compared with Duroc pigs. (a) Upregulated pathway by GO analysis in Tibetan pigs compared to Duroc pigs at MSC state. (b) Upregulated pathway by GO analysis in Tibetan pigs compared to Duroc pigs at ASC state. (c) Upregulated pathway by GO analysis in Tibetan pigs compared to Duroc pigs at preadipocytes state. (d) Upregulated pathway by GO analysis in Tibetan pigs compared to Duroc pigs at mature adipocyte state.

3.6 Tibetan pig SVF cells had higher adipogenic potential and fatty acid transport ability compared to Duroc pig SVF cells

To further validate the predictions mentioned above, we first assessed the proliferative capacity of SVF cells derived from Tibetan and Duroc pigs. We cultured SVF cells and detected the proliferation at 24, 48 and 72 h. This revealed that Duroc SVF cells had significantly higher proliferation capacity at 24, 48 and 72 h compared to Tibetan pig SVF cells, Fig. 6(a,b). However, *MKI67* and *CENPF* were not significantly different in expression at these time points between Tibetan pig and Duroc SVF cells Fig. S4(a,b). *MKI67* and *CENPF* were have been to mark proliferation cells in mice[38]. Then, we selected *TUBB6*, a significantly expressed gene in proliferation cell clusters in scRNA-seq, and found a significant higher in *TUBB6* expression in Duroc compared to Tibetan pig SVF cells at 24 and 72 h of proliferation, Fig. 6(c).

In addition, we assessed the adipogenic potential and metabolic capacity of ASC from Tibetan and Duroc pigs. The gene *CEBPA*, an early regulator of adipocyte differentiation, had higher expression in Tibetan pig SVF cells compared to Duroc pig SVF cells, Fig. 6(d). Additionally, genes related to fatty acid transport, such as *FABP4* and *CD36*, were significantly more expressed in Tibetan pig SVF cells than in Duroc pig SVF cells, Fig. 6(e).

Consistent with earlier findings that mitochondrial gene expression was higher in Duroc neck fat tissue, Fig. 1(e), we also observed higher *COX5B* expression in Duroc SVF cells compared to Tibetan pig SVF cells, Fig. 6(f).

The results suggested that SVF cells from Tibetan pigs had significantly higher adipogenic potential and fatty acid transport capability, while exhibiting lower proliferation and metabolic capacity compared to Duroc SVF cells.

3.7 Tibetan pigs have higher adipogenic capacity and lower metabolic activity than Duroc pigs at the mature adipocytes state

To further investigate the adipogenic process in Tibetan and Duroc pigs, we differentiated SVF cells into mature adipocytes by adipogenesis medium, and allowed them to differentiation until day 8. On day 8, oil red O staining revealed the presence of differentiated adipocytes in both Tibetan and Duroc cells, characterized by numerous lipid droplets. We quantified the lipid droplet content and found that mature adipocytes in Tibetan pigs had significantly higher lipid droplet content than in Duroc pigs, Fig. 7(a). Subsequently, we detected the expression of adipogenesis-related genes and observed that *CEBPA*, *CEBPB* and *ADIPOQ* were significantly higher in Tibetan mature adipocytes and *CD142* expression was lower than in Duroc pigs, Fig. 7(b). Similarly, we identified fatty acid transport genes and found that, compared to Duroc mature adipocytes, the expression of *FABP4* and *CD36* were significantly higher in mature adipocytes of Tibetan pigs, Fig. 7(c). It is suggested that Tibetan mature adipocytes provide stronger adipogenic and fatty acid transport capacity than Duroc pigs.

In addition, we evaluated cellular metabolic capability. It was observed that mature adipocytes of Tibetan pigs had lower expression of cytochrome complex genes *CYCS* and *COX5B* than in Duroc pigs (Fig. 7(d)). We further assessed energy metabolism in mature adipocytes by Seahorse experiments. While mature adipocytes of Tibetan and Duroc pigs did not differ in basal oxygen consumption rates and maximal mitochondrial oxygen consumption capacity Fig. S3(d), the mature adipocytes spare respiratory capacity of Tibetan pigs was lower than in Duroc pigs, Fig. 7(e).

4 Discussion

In this study, despite no morphological differences evident in white adipocytes between Tibetan and Duroc pigs, we found a stronger fat deposition capacity, with notably higher expression of adipogenesis genes. including *CEBPA*, *CEBPB* and *LEPTIN*, in Tibetan pigs. The evolutionary trajectories of Tibetan and Duroc pigs have led to distinct physiologic characteristics and adaptations. Tibetan pigs have gradually evolved into a breed emphasizing fat deposition, while Duroc pigs have been breed for lean meat production for commercial purposes. Previous research indicated that Tibetan pigs have thicker backfat and higher intramuscular fat content compared to Duroc pigs[19,22]. Additionally, Tibetan pigs have significantly higher expression of fat deposition-related genes such as *ADIPOQ* and *LEPTIN*[40].

In addition, it was found that Tibetan pigshad higher expression of *UCP3*, although their metabolism gene expression in adipose tissue was significantly lower compared to Duroc pigs. The absence of brown adipose tissue and the *UCP1* thermogenic gene in pigs leads to lower thermogenic capability[41]. Previous studies found cold-resistant pig breeds can activate non-shivering thermogenesis pathways through *UCP3* expression in cold environments, promoting adipocyte browning and aiding adaptation to harsh conditions[42]. In

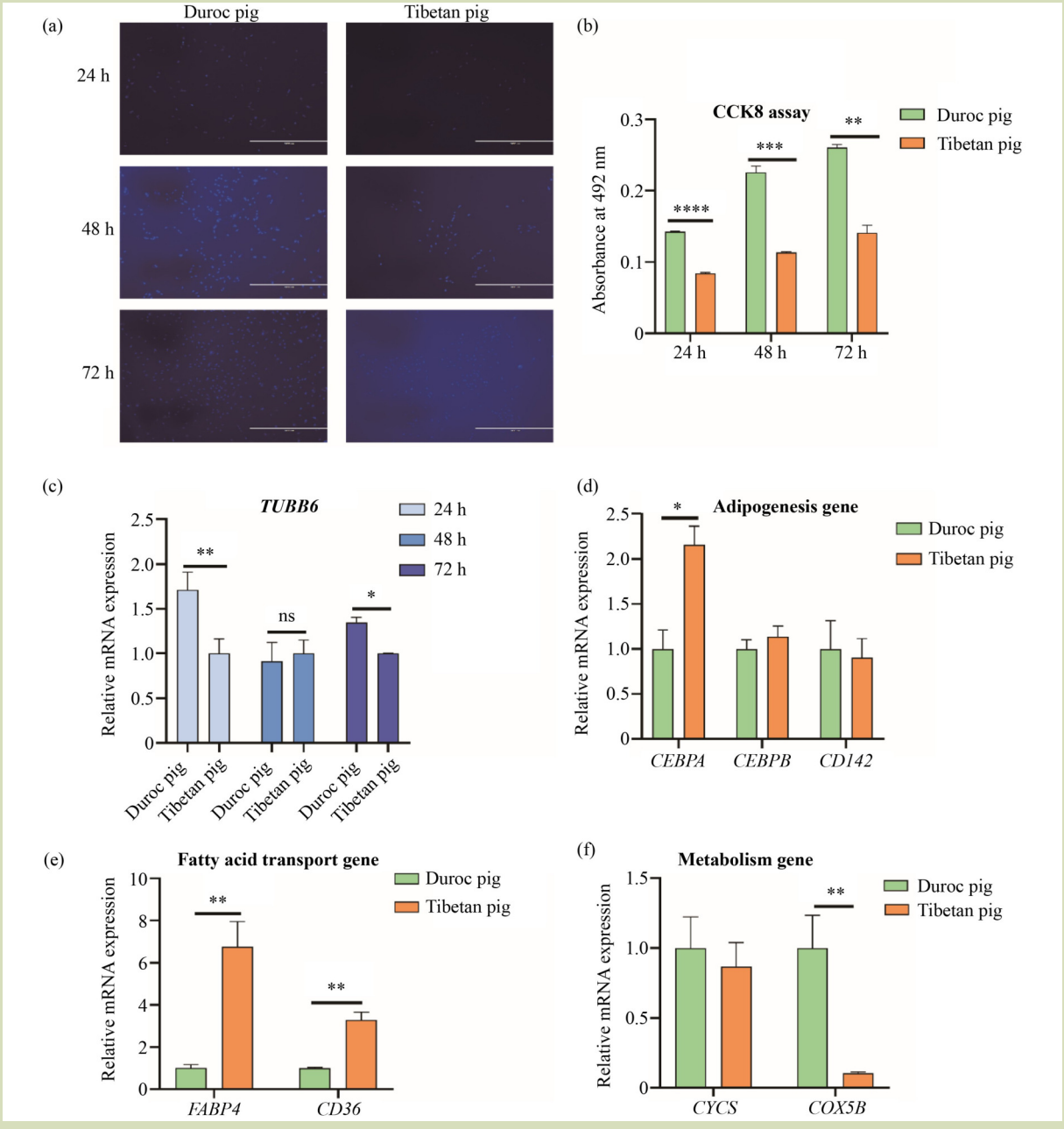

Fig. 6 Detection of cell proliferation and gene expression in SVF cells from neck WAT. (a) Hoechst staining on nuclei (blue) in SVF cells during cell cultured at 24, 48 and 72 h from Tibetan and Duroc pigs. (b) CCK8 assay of SVF cells during cell cultured at 24, 48 and 72 h from Tibetan and Duroc pigs. (c) Expression of proliferation gene *TUBB6* in SVF cells during cell cultured at 24, 48 and 72 h from Tibetan and Duroc pigs. (d) Expression of adipogenesis genes in SVF cells at day 0 during adipocyte differentiation from Tibetan and Duroc pigs. (e) Expression of fatty acid transport genes in SVF cells during adipocyte differentiation from Tibetan and Duroc pigs. (f) Expression of metabolism genes in SVF cells during adipocyte differentiation from Tibetan and Duroc pigs. For qPCR detection in each group, $n = 3$. Statistical significance was calculated on these mean values by *t*-test, * $P < 0.05$; ** $P < 0.01$.

addition, pigs also depend on shivering thermogenesis and physical measures, including clustering and optimizing husbandry conditions, to maintain body temperature in cold stress scenarios[43]. Previous study have shown that high-altitude animals and humans exhibit reduced oxygen sensitivity and decreased oxygen demand as adaptive responses to hypoxic environments[44]. These results further confirm Tibetan pigs possessed robust high-elevation adaptation.

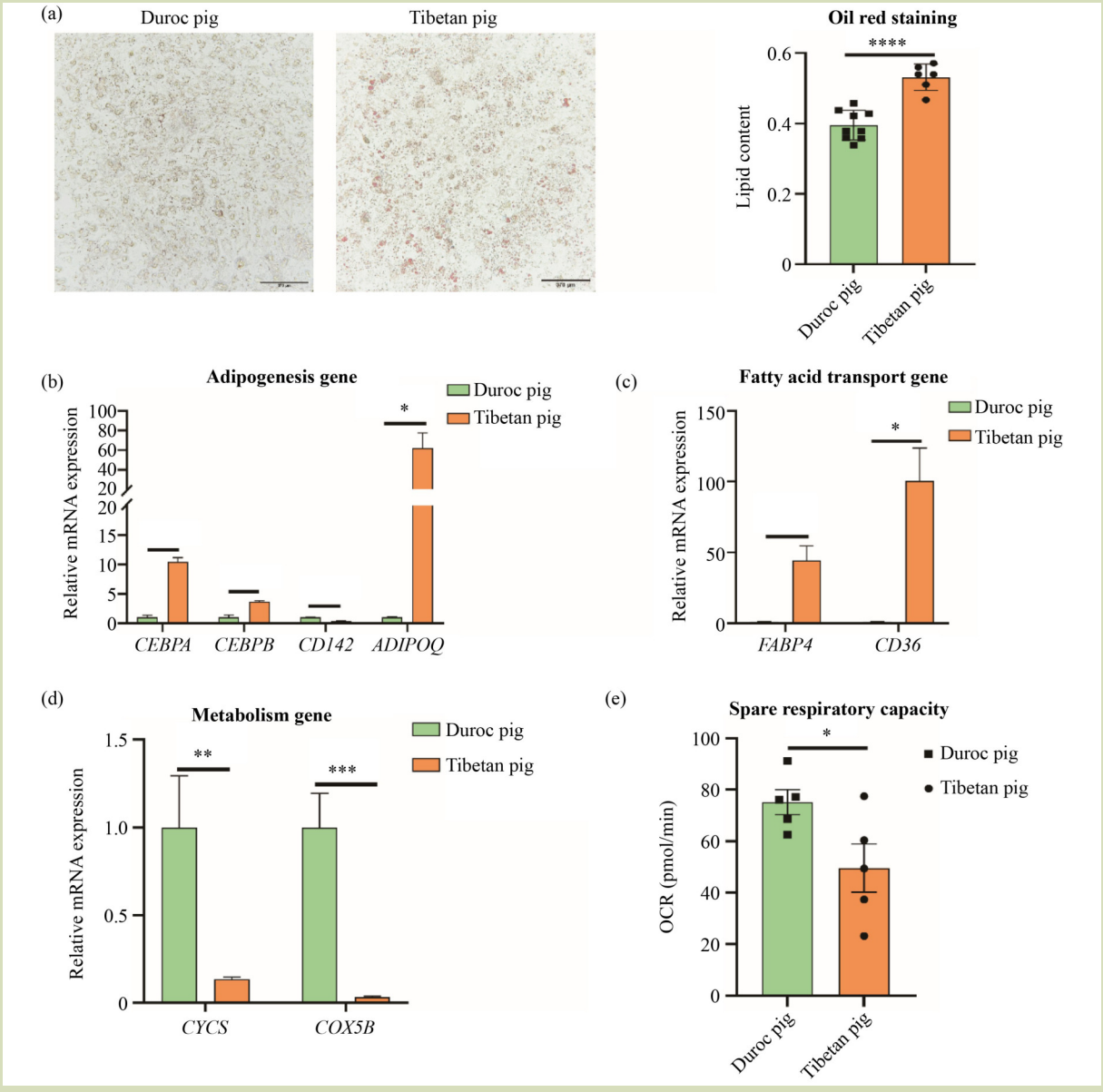

Fig. 7 Detection of cell adipogenesis capacity and gene expression in mature adipocytes during adipocyte differentiation. (a) Oil red O staining and lipid content in mature adipocytes on day 8 during adipocyte differentiation from Tibetan and Duroc pigs. (b) Expression of adipogenesis genes in mature adipocytes on day 8 during adipocyte differentiation from Tibetan and Duroc pigs. (c) Expression of fatty acid transport genes in mature adipocytes on day 8 during adipocyte differentiation from Tibetan and Duroc pigs. (d) Expression of metabolism genes in mature adipocytes on day 8 during adipocyte differentiation from Tibetan and Duroc pigs. (e) Detection of oxygen consumption rate in mature adipocytes on day 8 during adipocyte differentiation from Tibetan and Duroc pigs by Seahorse. For qPCR detection in each group, $n = 3$. Statistical significance was calculated on these mean values by *t*-test, * $P < 0.05$; ** $P < 0.01$. For oxygen consumption rate detection in each group, $n = 5$ in mature adipocytes. Statistical significance was calculated on these mean values by *t*-test, * $P < 0.05$.

However, the adipocyte development and metabolism regulation in fat- and lean-type pigs remain unclear. Therefore, we performed scRNA-seq analysis on the SVF cells of WAT from 4-day-old Tibetan and Duroc pigs to investigate heterogeneity of SVF cells and the adipocyte differentiation process in these pigs. We found in addition to clusters associated with adipocyte development, including mesenchymal stem cells (MSC), adipose stem cells (ASC), preadipocytes, proliferation cells and mature adipocytes, there are about 10% less endothelial cells and fewer myoblasts, VEC, vascular smooth muscle cells, and macrophages in adipose tissue. As previously described, adipose tissue is composed of

many types of cells, but adipose cells predominant. Consistent with the results of mouse white adipose SVF cells, there are different types of cells in the SVF cells of porcine white adipose tissue, but the types of immune cells were fewer than in mice[38].

In addition, compared to Duroc pigs, mature adipocyte proportions were found to be significantly higher in Tibetan pigs. The pseudo-time analysis indicated that Tibetan pig adipocyte stem cells differentiated into mature adipocytes during the differentiation process, with fewer cells remaining in the preadipocytes state. In contrast, in Duroc pigs, the majority of cells remained in the preadipocytes state without differentiation into mature adipocyte. Adipocytes undergo three main processes during differentiation. First, the MSC that have the potential to differentiate into various cell types and perhaps committed differentiation into preadipocytes. Subsequent proliferation and differentiation of preadipocytes, regulated by transcription factors such as *PPARG*, *CEBPA* and *CEBPB*, led to the formation of mature adipocytes. Lastly, some mature adipocytes re-entered the cell cycle, replenishing new cells to continue growing in adipose tissue[40,45,46]. It is suggested that Tibetan pig adipocyte stem cells once differentiated into preadipocytes more easily and more rapidly differentiated into mature adipocytes than in Duroc pigs. Additionally, the higher expression of adipogenic genes in Tibetan pig adipose tissue further indicates the higher adipogenic capacity of Tibetan pig preadipocytes to contribute to the lipid accumulation.

Subsequent GO analysis revealed that, compared to pathways upregulated in Duroc pigs, which mainly involved immune response processes such as innate immune response and oxidative stress response, Tibetan pigs enhanced pathways related to fatty acid transporters and fatty acid formation. In MSC, ASC and preadipocytes states, Tibetan pigs also had an upregulated thermogenic pathway, consistent with the high-elevation adaptive phenotype and cold resistance properties of these pigs. In Tibetan pigs, fatty acid oxidation consumes fuel for glucose oxidation and glycolysis processes, thereby reducing the demand for oxygen. Simultaneously, they accumulated more unsaturated fatty acids, which provides greater cold tolerance and is thus an adaptation for the harsh environment of high-elevation coldness[26,44]. In addition, the enhanced positive regulation of the lipid localization pathway at the preadipocytes stage further confirmed that Tibetan pig preadipocytes more readily progress toward maturity.

ASC in SVF cells from pig adipose tissue can differentiate into preadipocytes to ultimately become mature adipocytes *in vitro*[47]. In this study, we cultured white adipose SVF cells for 3 days and observed that the adipogenic ability and fatty acid transport capacity were significantly higher in Tibetan pigs than in Duroc pigs. This revealed the activation of the fatty acid transport pathway during the differentiation process of Tibetan pig ASC. However, SVF cells in Duroc pigs had higher proliferative capacity at 24, 48 and 72 h of culture. In the analysis of proliferative gene expression, *TUBB6* was expressed substantively more in the proliferation cluster of SVF cells in Duroc pigs than in Tibetan pigs. In contrast, the expression of proliferative markers *MKI67* and *CENPF* did not differ between Duroc and Tibetan pigs[38,48]. These results indicate that *TUBB6* can serve as an indicator of proliferation in pig SVF cells. Similarly, the metabolic capacity of ASC in Duroc pigs remained higher than in Tibetan pigs, indicating that Tibetan pigs have lower respiratory metabolic capacity at the adipose stem cell stage.

At the mature adipocyte stage (on day 8), Tibetan pigs also had higher adipogenic capabilities than Duroc pigs. Additionally, in comparison to the SVF stage, Tibetan pigs had greater abilities in fat formation and fatty acid transport than Duroc pigs. Consistent with earlier pseudo-time analysis results, Tibetan pig preadipocytes more readily progressed toward mature adipocytes. Additionally, the expression of *CD142*, a marker gene for preadipocytes[38], was significantly higher in Duroc pigs than in Tibetan pigs, and was consistent with the proportion of preadipocytes in Duroc pigs being higher than in Tibetan pigs as revealed by scRNA-seq analysis. At the mature adipocyte stage, the metabolic capacity and oxygen consumption rate of Tibetan pig cells remained lower than those of Duroc pigs. This indicates that Tibetan pig adipocytes have lower oxygen demand during the initial stages of differentiation, while maintaining consistently higher adipogenic and fatty acid transport capability than Duroc pigs. This highlights the enduring high-elevation adaptability of Tibetan pig during the differentiation process of ASC differentiation to mature adipocytes.

This study primarily focused on the developmental characteristics and cellular heterogeneity of adipose tissue in piglets. However, a comprehensive understanding of the epigenetic regulatory mechanisms underlying adipocyte development is still lacking. Also, there is a lack of direct evidence linking SVF cells differentiation into adipocyte formation and fat deposition in adult pigs. In future studies, it will be important to undertake single-nucleus ATAC-seq (snATAC-seq) analysis on adipose tissues from Tibetan and Duroc pigs to elucidate the epigenetic regulatory landscape of adipogenesis. In addition, there would be merit in examining the *in vivo* relationship between SVF cells fate determination and fat deposition in adult pigs.

5 Conclusions

In the present study, we observed that Tibetan pigs had greater adipogenic and fatty acid transport capabilities, but with a lower metabolic rate than Duroc pigs *in vitro* and *in vivo*. Our scRNA-seq results revealed the heterogeneity of subcutaneous adipose tissue SVF cells in the high-elevation fat deposition pig breed compared to the lean meat pig breed. Our study holds significant implications for guiding efforts to enhance the fat content and backfat thickness in agricultural animals.

Supplementary materials

The online version of this article at https://doi.org/10.15302/J-FASE-2025637 contains supplementary materials (Figs. S1–S4; Tables S1–S4).

Acknowledgements

This work was funded by the National Agricultural Biological Breeding Project of China. We extend our appreciation to Yunnan Agricultural University for supplying Tibetan pigs and providing a conducive environment for sample collection.

Compliance with ethics guidelines

Jiaping Li, Sa Li, Ning Li, and Xiaoxiang Hu declare that they have no conflicts of interest or financial conflicts to disclose. This article does not contain any studies with human or animal subjects performed by any of the authors.

REFERENCES

1. Mersmann H J, Smith S B. Development of white adipose tissue lipid metabolism. In: Burrin D G, Mersmann H J, eds. Biology of Growing Animals. Amsterdam: *Elsevier*, 2005, **3**: 275–302
2. Morigny P, Boucher J, Arner P, Langin D. Lipid and glucose metabolism in white adipocytes: pathways, dysfunction and therapeutics. *Nature Reviews. Endocrinology*, 2021, **17**(5): 276–295
3. Sarjeant K, Stephens J M. Adipogenesis. *Cold Spring Harbor Perspectives in Biology*, 2012, **4**(9): a008417
4. Kajimura S, Saito M. A new era in brown adipose tissue biology: molecular control of brown fat development and energy homeostasis. *Annual Review of Physiology*, 2014, **76**(1): 225–249
5. Wang W S, Seale P. Control of brown and beige fat development. *Nature Reviews. Molecular Cell Biology*, 2016, **17**(11): 691–702
6. Ailhaud G, Grimaldi P, Negrel R. Cellular and molecular aspects of adipose tissue development. *Annual Review of Nutrition*, 1992, **12**(1): 207–233
7. Cinti S. The adipose organ. *Prostaglandins, Leukotrienes, and Essential Fatty Acids*, 2005, **73**(1): 9–15
8. Nedergaard J, Cannon B. The browning of white adipose tissue: some burning issues. *Cell Metabolism*, 2014, **20**(3): 396–407
9. Harms M, Seale P. Brown and beige fat: development, function and therapeutic potential. *Nature Medicine*, 2013, **19**(10): 1252–1263
10. Louveau I, Perruchot M H, Bonnet M, Gondret F. Invited review: pre- and postnatal adipose tissue development in farm animals: from stem cells to adipocyte physiology. *Animal*, 2016, **10**(11): 1839–1847
11. Farmer S R. Transcriptional control of adipocyte formation. *Cell Metabolism*, 2006, **4**(4): 263–273
12. Kajimura S, Seale P, Spiegelman B M. Transcriptional control of brown fat development. *Cell Metabolism*, 2010, **11**(4): 257–262
13. Witkowska-Zimny M, Walenko K. Stem cells from adipose tissue. *Cellular & Molecular Biology Letters*, 2011, **16**(2): 236–257
14. Robledo F, Gonzalez-Hodar L, Tapia P, Figueroa A M, Ezquer F, Cortes V. Spheroids derived from the stromal vascular fraction of adipose tissue self-organize in complex adipose organoids and secrete leptin. *Stem Cell Research & Therapy*, 2023, **14**(1): 70
15. Min S Y, Desai A, Yang Z, Sharma A, Desouza T, Genga R M J, Kucukural A, Lifshitz L M, Nielsen S, Scheele C, Maehr R, Garber M, Corvera S. Diverse repertoire of human adipocyte subtypes develops from transcriptionally distinct mesenchymal progenitor cells. *Proceedings of the National Academy of Sciences of the United States of America*, 2019, **116**(36): 17970–17979
16. Divoux A, Whytock K L, Halasz L, Hopf M E, Sparks L M, Osborne T F, Smith S R. Distinct subpopulations of human subcutaneous adipose tissue precursor cells revealed by single-cell RNA sequencing. *American Journal of Physiology. Cell Physiology*, 2024, **326**(4): C1248–C1261
17. Berg F, Gustafson U, Andersson L. The uncoupling protein 1

gene (UCP1) is disrupted in the pig lineage: a genetic explanation for poor thermoregulation in piglets. *PLOS Genetics*, 2006, **2**(8): e129

18. Yan E F, Tan M Y, Jiao N, He L J, Wan B Y, Zhang X, Yin J D. Lysine 2-hydroxyisobutyrylation levels determined adipogenesis and fat accumulation in adipose tissue in pigs. *Journal of Animal Science and Biotechnology*, 2024, **15**(1): 99
19. Wu X D, Xiang D C, Zhang W, Ma Y, Zhao G Y, Yin Z J. Identification of breed-specific SNPs of Danish large white pig in comparison with four Chinese local pig breed genomes. *Genes*, 2024, **15**(5): 623
20. Zhang J, Chai J, Luo Z G, He H, Chen L, Liu X Q, Zhou Q F. Meat and nutritional quality comparison of purebred and crossbred pigs. *Animal Science Journal*, 2018, **89**(1): 202–210
21. Cabling M M, Kang H S, Lopez B M, Jang M, Kim H S, Nam K C, Choi J G, Seo K S. Estimation of genetic associations between production and meat quality traits in Duroc pigs. *Asian-Australasian Journal of Animal Sciences*, 2015, **28**(8): 1061–1065
22. Sarmiento-Garcia A, Vieira-Aller C. Improving fatty acid profile in native breed pigs using dietary strategies: a review. *Animals*, 2023, **13**(10): 1696
23. Nakajima I, Oe M, Ojima K, Muroya S, Shibata M, Chikuni K. Cellularity of developing subcutaneous adipose tissue in Landrace and Meishan pigs: adipocyte size differences between two breeds. *Animal Science Journal*, 2011, **82**(1): 144–149
24. Mourot J, Kouba M, Bonneau M. Comparative study of *in vitro* lipogenesis in various adipose tissues in the growing meishan pig: comparison with the large white pig (*Sus domesticus*). *Comparative Biochemistry and Physiology. Part B, Biochemistry & Molecular Biology*, 1996, **115**(3): 383–388
25. Poklukar K, Candek-Potokar M, Batorek Lukac N, Tomazin U, Skrlep M. Lipid deposition and metabolism in local and modern pig breeds: a review. *Animals*, 2020, **10**(3): 424
26. Merrick D, Sakers A, Irgebay Z, Okada C, Calvert C, Morley M P, Percec I, Seale P. Identification of a mesenchymal progenitor cell hierarchy in adipose tissue. *Science*, 2019, **364**(6438): eaav2501
27. Oguri Y, Shinoda K, Kim H, Alba D L, Bolus W R, Wang Q, Brown Z, Pradhan R N, Tajima K, Yoneshiro T, Ikeda K, Chen Y, Cheang R T, Tsujino K, Kim C R, Greiner V J, Datta R, Yang C D, Atabai K, Mcmanus M T, Koliwad S K, Spiegelman B M, Kajimura S. CD81 controls beige fat progenitor cell growth and energy balance via FAK signaling. *Cell*, 2020, **182**(3): 563–577.e520.
28. Vijay J, Gauthier M F, Biswell R L, Louiselle D A, Johnston J J, Cheung W A, Belden B, Pramatarova A, Biertho L, Gibson M, Simon M M, Djambazian H, Staffa A, Bourque G, Laitinen A, Nystedt J, Vohl M C, Fraser J D, Pastinen T, Tchernof A, Grundberg E. Single-cell analysis of human adipose tissue identifies depot and disease specific cell types. *Nature Metabolism*, 2020, **2**(1): 97–109
29. Zeisel A, Munoz-Manchado A B, Codeluppi S, Lonnerberg P, La Manno G, Jureus A, Marques S, Munguba H, He L Q, Betsholtz C, Rolny C, Castelo-Branco G, Hjerling-Leffler J, Linnarsson S. Brain structure. Cell types in the mouse cortex and hippocampus revealed by single-cell RNA-seq. *Science*, 2015, **347**(6226): 1138–1142
30. Wang M, Liu X X, Chang G, Chen Y D, An G, Yan L Y, Gao S, Xu Y W, Cui Y L, Dong J, Chen Y H, Fan X Y, Hu Y Q, Song K, Zhu X H, Gao Y, Yao Z K, Bian S H, Hou Y, Lu J H, Wang R, Fan Y, Lian Y, Tang W H, Wang Y P, Liu J Q, Zhao L M, Wang L Y, Liu Z T, Yuan R P, Shi Y J, Hu B Q, Ren X L, Tang F C, Zhao X Y, Qiao J. Single-Cell RNA sequencing analysis reveals sequential cell fate transition during human spermatogenesis. *Cell Stem Cell*, 2018, **23**(4): 599–614.e4.
31. Jia G S, Preussner J, Chen X, Guenther S, Yuan X J, Yekelchyk M, Kuenne C, Looso M, Zhou Y G, Teichmann S, Braun T. Single cell RNA-seq and ATAC-seq analysis of cardiac progenitor cell transition states and lineage settlement. *Nature Communications*, 2018, **9**(1): 4877
32. Cannon B, Nedergaard J. Cultures of adipose precursor cells from brown adipose tissue and of clonal brown-adipocyte-like cell lines. *Methods in Molecular Biology*, 2001, **155**: 213–224
33. Jang E, Shin M H, Kim K S, Kim Y, Na Y C, Woo H J, Kim Y, Lee J H, Jang H J. Anti-lipoapoptotic effect of Artemisia capillaris extract on free fatty acids-induced HepG2 cells. *BMC Complementary and Alternative Medicine*, 2014, **14**(1): 253
34. Ma X R, Wang D M, Zhao W J, Xu L Y. Deciphering the roles of PPARγ in adipocytes via dynamic change of transcription complex. *Frontiers in Endocrinology*, 2018, **9**: 473
35. Perruchot M H, Lefaucheur L, Barreau C, Casteilla L, Louveau I. Age-related changes in the features of porcine adult stem cells isolated from adipose tissue and skeletal muscle. *American Journal of Physiology. Cell Physiology*, 2013, **305**(7): C728–C738
36. Zimmerlin L, Donnenberg V S, Rubin J P, Donnenberg A D. Mesenchymal markers on human adipose stem/progenitor cells. *Cytometry. Part A*, 2013, **83A**(1): 134–140
37. Bourin P, Bunnell B A, Casteilla L, Dominici M, Katz A J, March K L, Redl H, Rubin J P, Yoshimura K, Gimble J M. Stromal cells from the adipose tissue-derived stromal vascular fraction and culture expanded adipose tissue-derived stromal/stem cells: a joint statement of the International Federation for Adipose Therapeutics and Science (IFATS) and the International Society for Cellular Therapy (ISCT). *Cytotherapy*, 2013, **15**(6): 641–648
38. Burl R B, Ramseyer V D, Rondini E A, Pique-Regi R, Lee Y H, Granneman J G. Deconstructing adipogenesis induced by beta3-adrenergic receptor activation with single-cell expression profiling. *Cell Metabolism*, 2018, **28**(2): 300–309.e4.
39. Dani V, Bruni-Favier S, Chignon-Sicard B, Loubat A, Doglio A, Dani C. Regulation of adipose progenitor cell expansion in a novel micro-physiological model of human adipose tissue mimicking fibrotic and pro-inflammatory microenvironments. *Cells*, 2022, **11**(18): 2798
40. Yang Loureiro Z, Solivan-Rivera J, Corvera S. Adipocyte heterogeneity underlying adipose tissue functions. *Endocrinology*, 2022, **163**(1): bqab138

41. Hou L J, Shi J, Cao L B, Xu G L, Hu C Y, Wang C. Pig has no uncoupling protein 1. *Biochemical and Biophysical Research Communications*, 2017, **487**(4): 795–800
42. Lin J, Cao C W, Tao C, Ye R C, Dong M, Zheng Q T, Wang C, Jiang X X, Qin G S, Yan C G, Li K, Speakman J R, Wang Y F, Jin W Z, Zhao J G. Cold adaptation in pigs depends on UCP3 in beige adipocytes. *Journal of Molecular Cell Biology*, 2017, **9**(5): 364–375
43. Young B A. Cold stress as it affects animal production. *Journal of Animal Science*, 1981, **52**(1): 154–163
44. Zhao P F, Li S B, He Z H, Ma X. Physiological and genetic basis of high-altitude indigenous animals' adaptation to hypoxic environments. *Animals*, 2024, **14**(20): 3031
45. Luo P H, Cao Y F, Luo L. Analysis of factors affecting fat deposition in pigs. *Xinjiang Animal Husbandry*, 2025, **41**(1): 9–12 (in Chinese)
46. Rosen E D, Macdougald O A. Adipocyte differentiation from the inside out. *Nature Reviews. Molecular Cell Biology*, 2006, **7**(12): 885–896
47. Gondret F, Pere M C, Tacher S, Dare S, Trefeu C, Le Huerou-Luron I, Louveau I. Spontaneous intra-uterine growth restriction modulates the endocrine status and the developmental expression of genes in porcine fetal and neonatal adipose tissue. *General and Comparative Endocrinology*, 2013, **194**: 208–216
48. Graefe C, Eichhorn L, Wurst P, Kleiner J, Heine A, Panetas I, Abdulla Z, Hoeft A, Frede S, Kurts C, Endl E, Weisheit C K. Optimized Ki-67 staining in murine cells: a tool to determine cell proliferation. *Molecular Biology Reports*, 2019, **46**(4): 4631–4643